GiG Research Institute

JOURNAL OF SUSTAINABLE MINING

Volume 22 | Issue 4 Article 6

2023

Influence of explosive maximum instantaneous charge on blasting environmental impact

Author(s) ORCID Identifier:
Olukemi Yetunde Odeyemi: 0000-0002-0922-2561
Blessing Olamide Taiwo: 0000-0002-6168-1300
Olarewaju Alaba: 0000-0002-2534-8551

Recommended Citation

Odeyemi, Olukemi Yetunde; Taiwo, Blessing Olamide; and Alaba, Olarewaju (2023) "Influence of explosive maximum instantaneous charge on blasting environmental impact," *Journal of Sustainable Mining*: Vol. 22 : Iss. 4 , Article 6.
Available at: https://doi.org/10.46873/2300-3960.1398

Influence of explosive maximum instantaneous charge on blasting environmental impact

Abstract

Our research looked at the effect of explosive maximum instantaneous charge on ground vibrations and noise levels during blasting operations at the Calaba limestone quarry in Nigeria. Vibrock (V9000) seismograph was used to take readings related to ground vibrations and noise generated during all blasting operations that took place in the quarry for a period of one year. The results obtained indicate that the average ground vibration readings fall between 0.25mm/s to 3.6mm/s and the average noise decibel generated during the blasting operations between 35 to 158 dB. An artificial neural network (ANN) model is developed in this study for the prediction of blast-induced ground vibration and noise level. The proposed ANN model was compared with existing empirical models and was found to give the highest prediction accuracy. It was revealed that both noises generated and ground vibrations during all blasting operations increase with an increase in explosive maximum instantaneous charge. Additionally, the measuring equipment distance from the blast site was also revealed to have a negative correlation with noise generated and ground vibrations.

Keywords

blasting, explosive energy, blast ground vibration, maximum instantaneous charge, seismograph

RESEARCH ARTICLE

Influence of explosive maximum instantaneous charge on blasting environmental impact

Olukemi Y. Odeyemi, Blessing O. Taiwo*, Olarewaju C. Alaba

Federal University of Technology Akure, Mining Engineering, Nigeria

Abstract

Our research looked at the effect of explosive maximum instantaneous charge on ground vibrations and noise levels during blasting operations at the Calaba limestone quarry in Nigeria. Vibrock (V9000) seismograph was used to take readings related to ground vibrations and noise generated during all blasting operations that took place in the quarry for a period of one year. The results obtained indicate that the average ground vibration readings fall between 0.25 mm/s to 3.6 mm/s and the average noise decibel generated during the blasting operations between 35 and 158 dB. An artificial neural network (ANN) model is developed in this study for the prediction of blast-induced ground vibration and noise level. The proposed ANN model was compared with existing empirical models and was found to give the highest prediction accuracy. It was revealed that both noises generated and ground vibrations during all blasting operations increase with an increase in explosive maximum instantaneous charge. Additionally, the measuring equipment distance from the blast site was also revealed to have a negative correlation with noise generated and ground vibrations.

Keywords: blasting, explosive energy, blast ground vibration, maximum instantaneous charge, seismograph

1. Introduction

Blasting operations are commonly used in many quarries to liberate in-situ rock mass and ensure material availability [1]. The blasting operation is carried out by drilling holes of varying diameters and lengths and filling these holes with a blasting agent of choice. According to Jhanwar [2], the primary goal of this operation is to provide enough energetic wave energy to cause the fracturing of rock mass into smaller sizes. Explosives energy is rated in a variety of ways, obtained either from calculation or from experimental tests. However, the questions of what amount of that explosive energy is transferred to the rock for fragmentation and what fraction of it is converted into efficient work in the usual mining application of rock blasting remain largely undefined. Although the measurement of some of the effects of the explosive excess energy usage has been explained to be for vibration, fragmentation and rock movement, they are usually conducted for blast control purpose, and the results are usually important to ensure a sustainable blasting environment. According to Bhandari 2013, blasting operation generates a nuisance effect if more fine fragments are produced and then when more dust is dispersed under explosion. When large amounts of fugitive dust are released into the environment uncontrollably, they can cause widespread nuisance and potential health concerns for on-site personnel and surrounding communities. Though the blasting dust plume is raised for a few minutes, the majority of the dust settles in and around the mining area, and some of it is dispersed before it settles. Depending on the explosive maximum charge quantity and the meteorological conditions, dust dispersal can travel long distances, endangering community health. The amount of fines and dust generated during blasting is determined by the type of explosives used and how they are charged in the hole. The blasting operation involves the detonation of a specific explosive quantity to fragment in-situ and oversize rock blocks for particle reduction [3]. A production blast is executed by drilling a series of blast holes into the rock mass and filling them with explosive

Received 23 September 2022; revised 11 January 2023; accepted 12 June 2023.
Available online 25 October 2023

* Corresponding author.
E-mail address: taiwoblessing199@gmail.com (B.O. Taiwo).

https://doi.org/10.46873/2300-3960.1398

materials confined by stemming and confining material. Rock blasting causes ground shock and vibration, which can damage nearby structures [4]. Because of the increased threat from various man-made activities, the minimization of blast-induced effects on natural and man-made structures has received considerable attention in recent decades [5,6]. The need to improve the environment of current mining areas, which are becoming increasingly difficult to manage due to the use of excessive explosive powder, has given rise to the need to study the response of blast damage and to build a soft computing mathematical model for the prediction of blast effect, allowing management personnel at various levels to control the ground vibration and blast-induced noise level, all with the goal of improving environmental safety performance. The most important parameters to investigate in air shock studies, according to Deniz and Deniz [7], are the amount of explosives used per delay time and the distance to the measuring station. This work proposed an artificial intelligence-based model for blast environmental impact that will guide mining engineers in mining companies and aid quarries and mines operators in promoting sustainable blasting practices. The first section of this paper examines the rock's moisture content and strength condition as a relationship factor, while the second section investigates the level of blast-induced ground vibration and noise generated by the mine operation to determine the environmental safety level relative to the standard threshold. In addition, the paper investigates the effect of maximum instantaneous charge and measuring instrument placement on blast-induced ground vibration and noise level in the case study limestone mine. As noted in the literature, generated blast-induced impact is dependent on the explosive charge per delay. This study also employs an Artificial Neural Network (ANN) approach based on field study results to mitigate the risk of blast-induced ground vibration and noise. Blast operation was monitored to measure blast-induced ground vibration and noise. The field test results for blast charge rate and observation distance will be used as input parameters in the proposed models, with blast impact as the desired output.

1.1. Description of the study area

A field study was conducted at a limestone quarry in Calaba to achieve the goal of this study.

The study area's geology consists of intercalated limestone and marl layers underlain by limestone

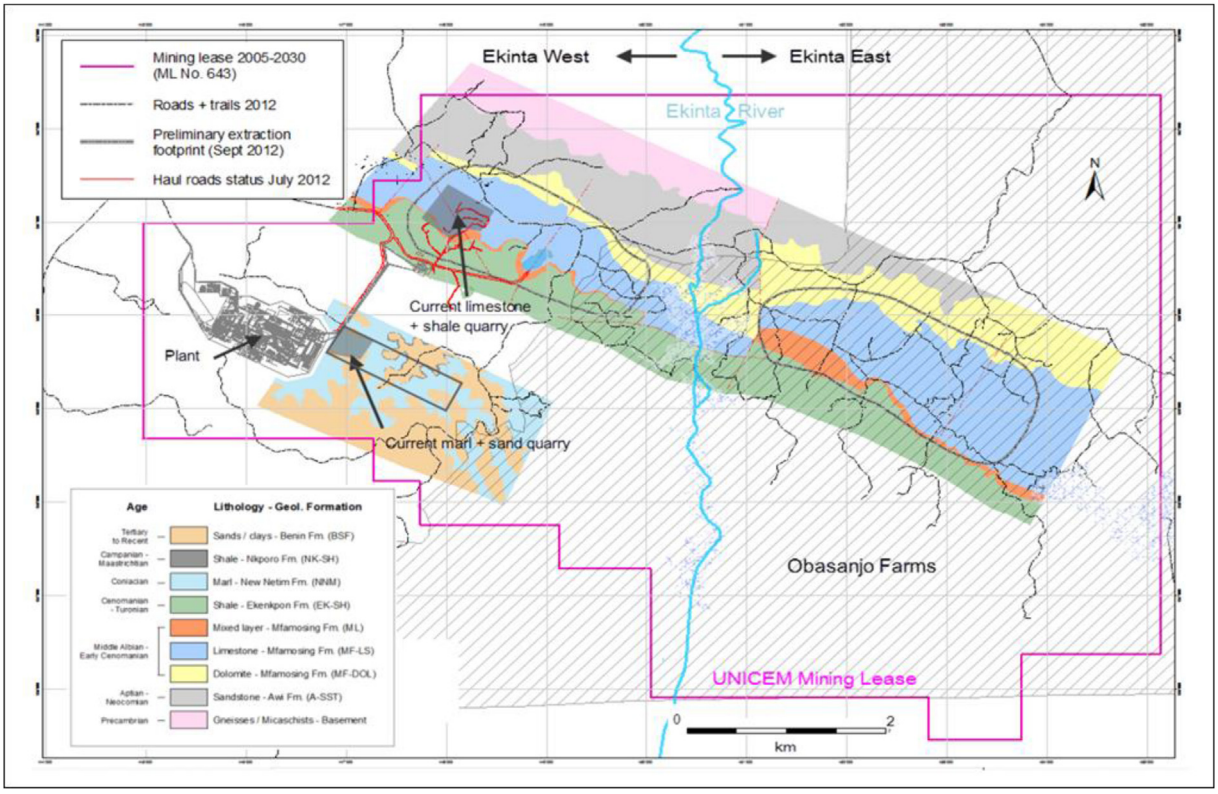

Fig. 1. Geological map of the case study area (modified after Unicem geological field mapping operation).

and dolomite from the Mfamosing formation, all of which date from the middle Albian to the early Cenomanian. As shown in Fig. 1, the limestone deposit in the case study quarry site outcropped in a valley with an approximate area cover of 779,140 m^2. The lowest and highest points on the ground are 20 and 50 m, respectively. The limestone quarry site's coordinates are 560,962 N and 448,015 E.

2. Literature review

According to Ainalis et al., explosive charge detonation involves a rapid and stable chemical reaction that travels through the explosive charge at its Velocity of Detonation and produces very high temperature and density gases [8]. They found that during blast charge detonation, the detonation velocity can range from 1500 to 9000 m/s, with equivalent detonation pressures ranging from 1 to 14 GPa. The explosive charge detonation process during rock blasting involves two distinct phenomena [9,10]. Cullis first explained that the rapid detonation of explosives creates a supersonic shock wave that travels through the explosive charge and causes rock fragmentation [11]. Second, the high-pressure gas that follows the shock wave enters the surrounding rock mass via existing or newly formed fractures. According to Resende et al., explosive shock waves are short-duration (a few milliseconds) waves that cause the blast hole to rapidly expand and contract, imparting pressure waves into the surrounding medium [12].

Dumakor-Dupey et al. [13] explained the utilization of explosive energy released during blast initiation. They noted that 70–80% of the explosive energy released produces undesirable outcomes, while 20–30% is used to fragment and throw rock material. The 70–80% explosive energy generates ground vibration, airblast/air overpressure, noise, heat, dust, and flyrock, among other undesirable outcomes. According to Jaffar et al. [14], vibration is the back-and-forth or repetitive motion of an object from its point of rest. When a force is applied to a mass, the particle constituents that make up the mass vibrate in response to the force [15]. When the force is removed, the particles' stored energy causes them to move upward through the position of rest to the upper elastic limit [14,15]. When a particle reaches its upper elastic limit, its mass comes to a halt and reverses direction, returning to the lower elastic limit via the position of rest [15]. Geometric spreading and frictional loss are the primary causes of vibration [16]. The decrease in vibration caused by the non-elasticity of rock and rock structure is dictated by frictional loss. Bansah et al. [17] also noted that ground vibrations and airblast resulting from blasting induce new cracks and also expand existing cracks which alter the stability of building and engineering structures. Airblast overpressure is an unavoidable byproduct of any blasting, with the primary components being vibration and venting. The overpressure is also linked to the formation of fly rock. Ground vibration is a technical term that describes mostly man-made vibrations of the ground, as opposed to natural vibrations studied by seismologists. Such vibration consists of that resulting from explosions, construction works, and railway and road transport [18]. The amount of vibration generated during a blasting operation is determined by the amount of explosive charge detonated per delay.

The work of Valdivia et al. and Rossmanith et al. revealed the importance of several variables whose changes can influence vibration reduction and blasting operation improvement [19,20].

Bhandari distinguished between controllable and uncontrollable factors influencing vibrations [21]. Controllable factors such as blast geometry, explosive type, steaming, priming, and initiation were also mentioned to influence blast fragmentation [3]. Other factors influencing ground vibration during blasting include rock strength, number of blast holes, and measuring distance to the blast site, to name a few. Production blasts are a complex phenomenon, with many factors influencing their performance and subsequent ground vibrations. The various blasting factors that have a minor and major influence on ground vibration during blast operation are presented by Banadaki and Mohanty (see Table 1) [22].

In their paper, Alessandro et al. presented Eq. (1) as a relationship between the blasting parameter and *PPV* [23].

$$t_{\text{det}} = \frac{N \cdot L}{VOD} \tag{1}$$

Where N is the number of explosive cartridges in the boreholes, L is the length of each cartridge in mm, and VOD is the velocity of detonation.

$$cpd = N \cdot L \cdot \phi^2 \cdot \frac{\pi}{2} \cdot \rho_e \tag{2}$$

Where ϕ is the charge diameter (mm); ρ_e is the explosive density in $kg \cdot m^{-3}$

From Eq. (2), Eq. (1) for calculating *PVV* becomes Eq. 3

Table 1. List of various factors and their influence on ground vibration from [8].

	Factor	Ground motion influence		
		Significant	Moderate	Insignificant
Factors within operator's control	Charge weight per delay	Yes		
	Delay interval	Yes		
	Burden and spacing		Yes	
	Amount of stemming			Yes
	Types of stemming			Yes
	Charge length and diameter			Yes
	Charge depth			Yes
	Angle of blast hole		Yes	
	Direction of initiation			Yes
	Charge weight per delay			Yes
	Charge confinement	Yes		
Factors out of site operator's control	General surface terrain			Yes
	Overburden type and depth	Yes		
	Wind and weather			Yes

$$ppv = \left[\frac{2 \cdot D^2 \cdot VOD^{\frac{1}{2}}}{N \cdot L \cdot \phi \cdot (\pi \cdot \rho_e)^{\frac{1}{2}}}\right]^n \quad (3)$$

Eq. (3) shows that *PPV* does not depend only on the charge per delay (*cpd*), but also on *VOD*. The properties of detonated explosives, in addition to an explosive weight initiated per delay, are very important in determining the vibration behavior of soils in a blast environment. Mpofu et al. also provide a thorough investigation into the various blasting parameters that influence ground vibration and air blast [24]. Uniaxial Compressive Strength, unit weight, density, Rock Quality Designation, and Geological Strength Index are some of the geotechnical properties that influence blasts to induce noise and vibration, according to Ranjan et al. [25]. Roy et al. [26] investigated the effect of Young's modulus and *P*-wave velocities on *PPV*. They unearthed that higher *P*-wave velocity causes more ground vibration and that higher Young's modulus rock has less attenuation, resulting in energy loss and an increase in ground vibration. For a long time, one of the methods used to reduce blast instantaneous charge weight in mines and quarries has been air decking. Cheng et al. investigated the effects of an axial air deck in a borehole on blast-induced ground vibrations. Nonetheless, the effect of maximum instantaneous charge on the most dangerous blast-after effect, blast-induced fly rock and ground vibration has not been clarified [27]. Several researchers also focused on the application of prediction techniques in improving blasting operation and minimizing blast-induced ground vibration and noise level, including [28–33].

3. Materials and methods

According to Etikan and Bala, purposeful sampling was used to collect representative samples from the case study limestone deposit. The case study rock formation yielded cylindrical core samples [33]. The moisture content, density, and uniaxial compressive strength (*UCS*) of the case study rock formation were determined using cylindrical samples. The testing machine used was a Riedligen (made in Germany) capable of loading up to 3000 kN at a rate that met the International Society of Rock Mechanics (ISRM) requirement [34]. The maximum instantaneous charge of each blast round was calculated per hole and multiplied by the total number of holes. The sequence of distribution of the detonating device is generated, and the firing sequence of each blast round was obtained, as shown in Fig. 2. The sequence with the largest number of holes was identified. The kilogram (kg) of explosives per hole was measured. The Maximum Instantaneous charge of each blast round was obtained using Eq. (4):

$$MIC = N \cdot W \quad (4)$$

Where *N* is the total number of instant holes blasted per delay, *MIC* is the maximum instantaneous charge in kg, and *W* is the explosive charge per hole.

Lafarge Cement Company (LCC) quarry is located in Calabar, Cross River State, and south-eastern Nigeria. The limestone quarry pits lie within latitude 5°4′39″ and longitude 8°31′54′′. The blast ground vibration measurement to cover the limestone quarry blasting point and active mining site. That is to have a good average of the response of rocks along the path of the waves induced by the

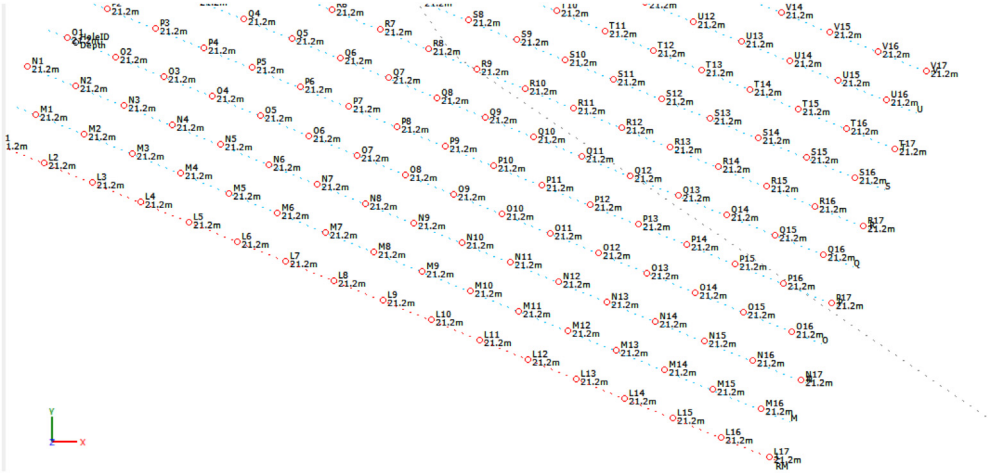

Fig. 2. Typical firing pattern used in the case study blasting operation.

blasts. Blast hole diameter ranges from 11.3 cm (4.5 inches) to 15 cm (6 inches). Other parameters of includes benches include burden = 6.5 m, spacing = 8.5 m, stemming length = 3 m, and sub drilling = 2 m. The explosive charge is ANFO, while Ammonia Gelatin dynamite has been used as priming, bottom, and boosting charges. The initiation type is a NONEL system in one row with a 25 ms surface delay interval. Understanding the responses of the blast effect due to explosive charge weight will assist in improving blast environmental sustainability and also enhance the safety of workers and mine machines.

To address this issue, seventy-five (75) full-scale production blasts covering one-year operations were considered in this study, with the number of blast holes per blast ranging from 30 to 62. The weight of the charge per delay ranged from 60 kg to 90 kg and the total charge weight per blast ranged from 580 kg to 1600 kg. The distance between the seismograph's locations to the center of the blast ranged from 128 to 1025 mm. The instruments used include one Vibrock (V9000) seismograph system (2 kg boxed weight) with an internet-based remote and GSM feature (see Fig. 3). The Vibrock V9000 seismograph is a completely independent unit. Seismographs have been used to record the ground vibrations and resultant peak noise during each blast. Distance from each seismograph location to the center of the blast has been measured in accordance with Stagg and Engler [35]. The results generated are interpreted and presented quantitatively and qualitatively using graphs; geotechnical parameters are correlated with measured noise and vibration to ascertain the effect of geology on noise and vibration. The study stepwise flow sheet is shown in Fig. 4 with the proposed sustainable model approach.

Fig. 3. Seismograph in position for noise and vibration measurement.

3.1. Artificial neural network (ANN) for the predictions of blast-induced impact

Adjusting the weights and biases of a trained ANN network is part of the process of making it more accurate. The correct weights and biases of the ANN model are typically determined using a number of methods. In this work, we used a hybrid algorithm with two transfer functions to train a network to its maximum potential (trainbr and trainlm). The proposed model was created with the help of 75 blast data samples gathered from in-field observations. To ensure that the models produced by these data sets were as accurate as possible, the dataset was normalized. When training the ANN model, datasets were arbitrarily split into three groups. In order to train the ANN model, 80% of the datasets were used, while the remaining 10% were

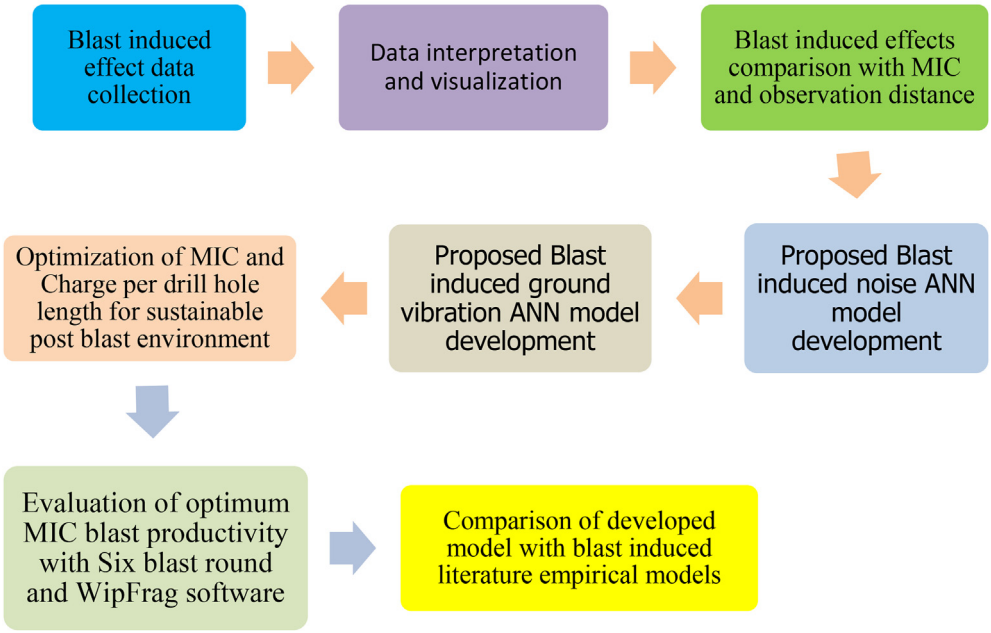

Fig. 4. A flowchart of the research work.

used for testing and validation. The ANN model was developed using MATLAB. In order to train the model network, we utilized hybrid, Bayesian, and Levenberg-Marquardt algorithms. Using the guidelines cited by Lawal et al. [36], a series of linear mathematical equations will be derived to represent the hybrid optimum model.

3.2. Analysis of the optimum MIC blast production sustainability with WipFrag software

In order to digitalize the contents of images, state-of-the-art image-based gravimetry image processing software, such as WipFrag, uses the grayscale technique [37]. WipFrag software was used to analyze six blast images taken from blast rounds designed with the proposed optimized MIC using the developed model. This allowed for the measurement of the blast fragment size distribution. All of the blast photos were taken using WipFrag's methods [38].

4. Results and discussion

The study was conducted using seventy-five production blasts involving the monitoring of the blast maximum instantaneous charge, ground vibration, and peak noise level.

4.1. Rock strength characteristics results

Table 2 presents the uniaxial compressive strength, density, and moisture content results of the three tests and the average value of the rock formations in the case study area. The Limestone formation as identified by the UCS result, has high strength with an average value of 90 MPa; the limestone is classified as strong limestone according to Bieniawski's [39] rock *UCS* rating. The formation has average moisture content and density value of 8.8 and 2.41 kg/m^3, respectively. Fig. 5 shows the relationship between the limestone formation strength and water content.

Table 2. Result of the rock strength properties.

Sample ID	Moisture content	Density (kg/m^3)	*UCS* (MPa)
1	8	2.36	85
2	9.5	2.46	88
3	9	2.4	99
Average	8.8	2.41	90

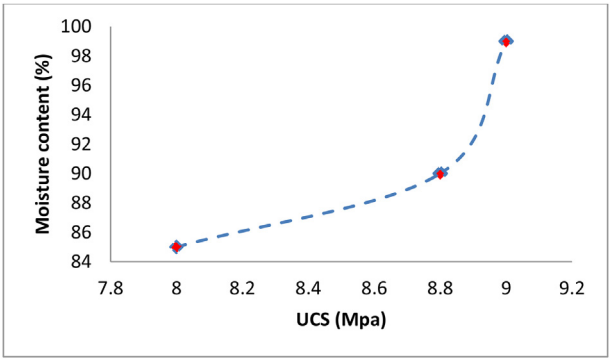

Fig. 5. Relationship between limestone UCS and moisture content.

Rock moisture content is the key factor determining the mine water infiltration rate. Low water content rock support the quick migration of mine water from the pit into the environment, which results in soil contamination in case of acid mine drainage [40]. The result of this study revealed that a positive correlation exists between limestone moisture content and strength property, with a continuous increase in moisture content percentage as the rock strength increases.

4.2. Result of maximum instantaneous charge, noise and ground vibration measured from the limestone quarry

The statistical analysis result of the measured and evaluated parameters obtained during field measurement is shown in Table 3. The average and range of the evaluated blasting resultant maximum instantaneous charge in the Limestone blast site, as well as the measured noise and ground vibration from the blasting operation using the Seismograph, were presented. The results show that the maximum initiated explosive charge, noise level, and ground vibration in the blast site range from 580 kg to 1600 kg, 35 dB–158 dB, and 0.25 mm/s to 3.6 mm/s, respectively. The obtained readings from the case study blast site are higher than the limits set by the Federal Environmental Protection Agency (FEPA) of 5.0 mm/s and 150 dB [41]. The readings were higher when compared with the result of the Ewekoro blasting operation as measured by [41]. The noise level was noted to fall beyond the permissible limits, which require adjustment so as to prevent damage to mine humans and contribute to metrological conditions such as wind speed and dust dispersion [42]. Machine learning modelling approach using an artificial neural network approach will be applied in section 4.3.1 to minimize the blast-induced noise level below the FEPA threshold.

4.3. Relationship between generated limestone blast noise level, the measuring equipment distance and MIC

To make proper adjustments to the blasting operation at the mine, this section proposes a linear and artificial intelligence-based mathematical equation for the prediction and optimization of blast-induced ground vibration and noise level. The relationship between maximum instantaneous charge weight, measuring equipment distance, and generated blast induced noise level is shown in Fig. 6. Considering the result, it was observed that blast-generated noise and the maximum instantaneous charge have a positive correlation (Fig. 6a). Additionally, it was also observed that the maximum instantaneous charge weight increases with increase in the level of blast-induced noise as shown in Fig. 5a. This result was noted to be a result

Table 3. Measured dataset statistics.

	MIC (kg)	Distance to instrument (m)	Noise (dB)	Ground vibration (mm/s)
Max	1600	1025	158.1	3.648
Min	580	128	35.74	0.25
Mean	1312.467	384.16	123.76	2.521
Mode	1500	262	146.14	3.248
variance	46,110.47	36,216.703	6.551	0.613
standard deviation	214.733	190.306	2.559	0.783

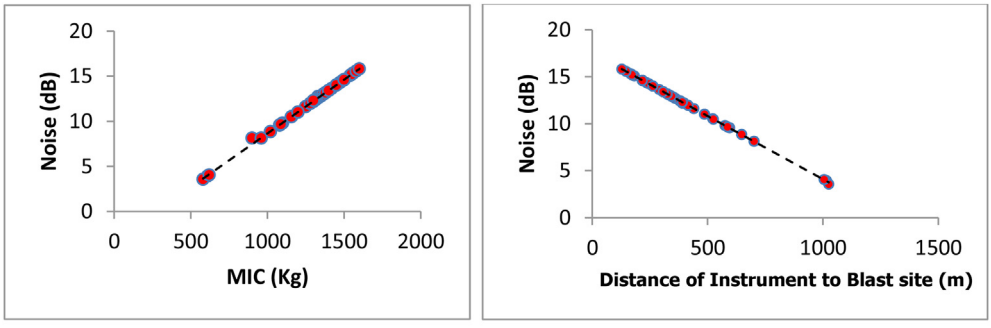

a. b.

Fig. 6. Relationship between the measure blasts generated noise and (a) instrument distance to blast site, and (b) MIC.

of the increase in the energy released by the charge weight at detonation due to the increased powder factor [43].

Fig. 6b shows that a negative correlation exists between the generated noise measured and the distance of the measuring instrument to the blast site. Fig. 5b also reveals that as the measuring distance increases the level of noise decreases. The blasting operation generated noise was found to be below the FEPA threshold level, making it safe for human occupation within the operating radius. Eqs. (5) and (6) express the linear relationship between the noise generated by a blast, the observation distance, and the maximum instantaneous charge per blast round, with R^2 values of 0.87 and 0.98, respectively.

$$N = -0.134 \cdot D + 175.4 \tag{5}$$

$$N = 0.12 \cdot MIC - 33.9 \tag{6}$$

Where: MIC is the maximum instantaneous charge in kg, N is the noise level in dB, and D is a distance of the instrument to the blast site in m.

4.3.1. Developed blast-induced noise ANN model

Revealing that the noise level generated from the case study mine is above the safety threshold level, as shown in section 4.2, the ANN model with 2:3:1 architecture was built based on the approach explained in section 3.1 using a hybrid algorithm. Fig. 7 presents the prediction regression for both the training and testing dataset. The model with $R^2 = 0.998$ and $MSE = 0.474$ was adopted for blast-induced noise prediction and obtaining the optimum charge weight per drill hole based on the MIC and the maximum safety distance. The blast-induced noise formula is found in Equations (7)–(10) by the best ANN model, where the R^2 values are 99.91% and 99.8% for the training and testing dataset, respectively. The proposed model was found suitable for predicting the noise level in a limestone quarry for pre-blast design.

$$N = 61.2 \tanh\left(\sum_{i=1}^{4} Xi + 0.842704\right) + 96.94 \tag{7}$$

$$X_1 = -1.01353\tanh\left(-2.338MIC - 0.96064D + 2.248951\right) \tag{8}$$

$$X_2 = 0.641155\tanh\left(-2.23583MIC + 0.72424D - 0.28067\right) \tag{9}$$

$$X_3 = 0.30836\tanh\left(1.217995MIC - 2.05348D + 2.43614\right) \tag{10}$$

4.4. Relationship between generated limestone blast ground vibration, measuring distance and MIC

Fig. 8 shows the relationships between the blasts' induced ground vibration, MIC, and the distance of

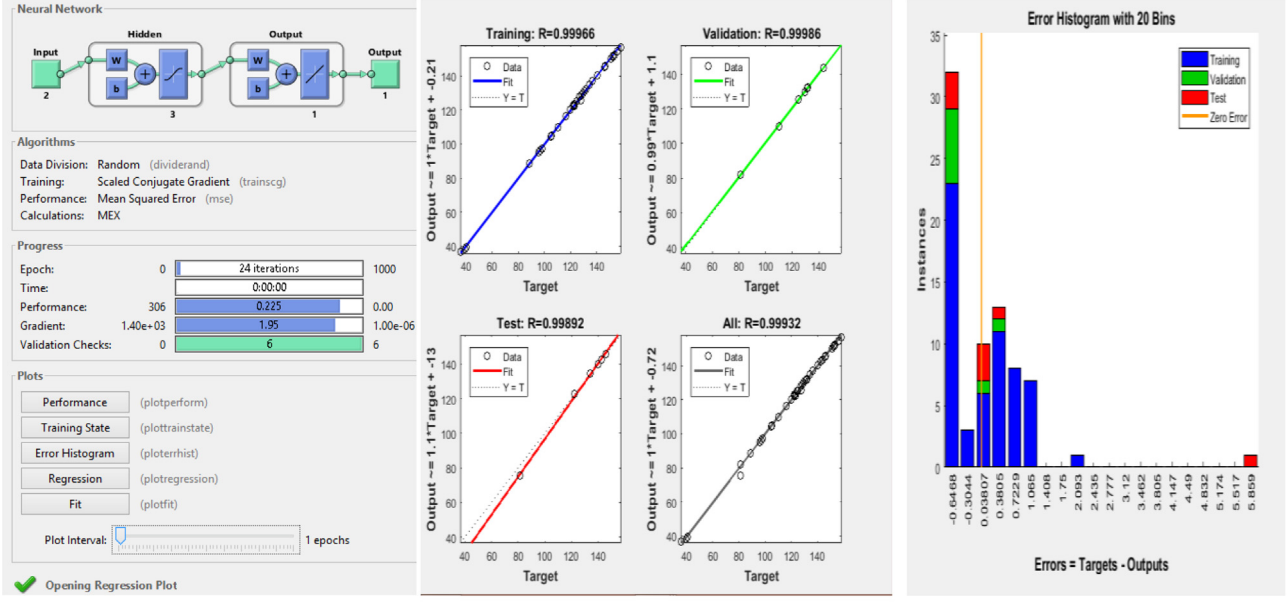

a. *b.* *c.*

Fig. 7. Blast-induced noise ANN model performance graph: model architecture (a), training and testing regression (b), model error histogram (c).

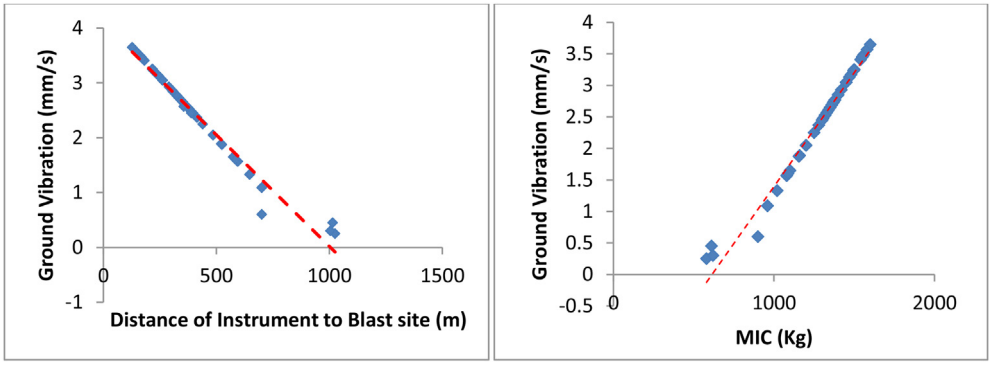

a. b.

Fig. 8. Relationship between the measure blasts generated ground vibration and (a) measuring the distance from the blast site, and (b) maximum Instantaneous charge.

the measuring instrument to the blast site. The ground vibration at the limestone quarry decreases with an increase in the instrument setup distance (See Fig. 8a), expressing a continuous decrease in the induced ground vibration with distance in relation to Zhi-qiang Yin et al. and Mesec et al. findings [44,45]. Fig. 8b shows the relationships between the blasts that induce ground vibration and the blast maximum instantaneous charge (*MIC*). The ground vibration level shows an increasing trend with an increase in the maximum instantaneous charge initiated at once in the blast site. The result shows that the rate of ground vibration depends on the explosive energy usage in the quarry, which also depends on the *MIC*.

Eqs. (7) and (8) shows the linear relationship between the *MIC*, blast site distance and ground vibration measured. The obtained R^2 values are 0.97 and 0.89, respectively; it is suitable for predicting the blast-induced ground vibration in a limestone quarry.

$$GV = 0.003 \cdot \mathrm{MIC} - 2.218 \tag{7a}$$

$$GV = -0.004 \cdot D + 4.083 \tag{8a}$$

Where: *GV* is the ground vibration in mm/s, *MIC* is the maximum instantaneous charge in kg, and *D* is the distance of the instrument to the blast site in m.

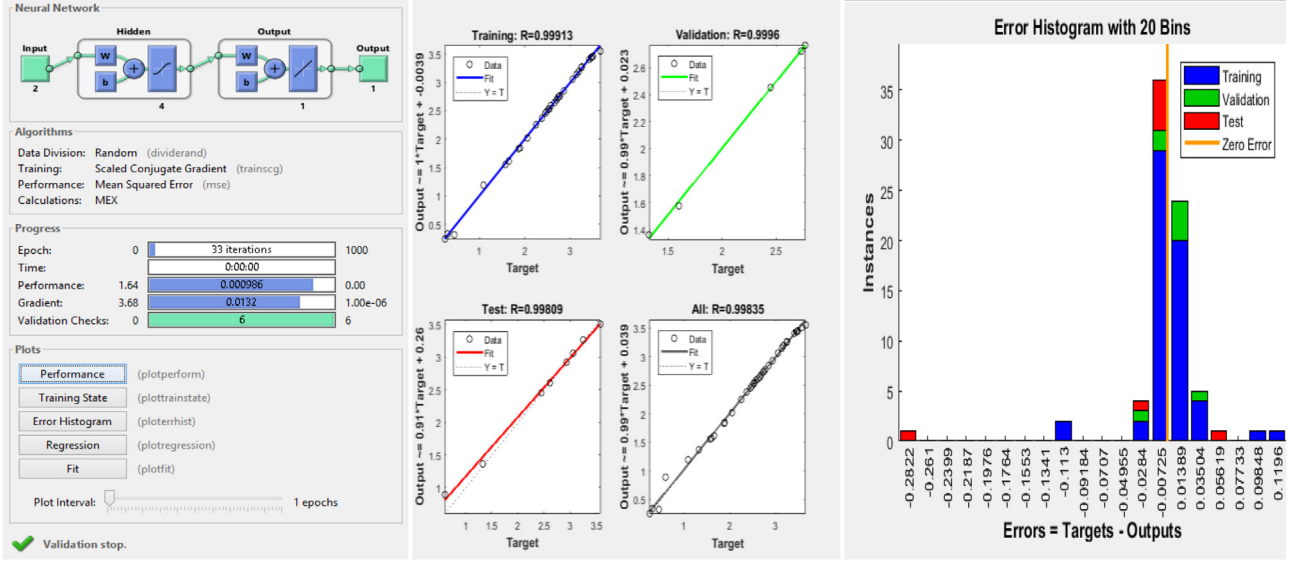

a. b. c.

Fig. 9. Blast-induced vibration ANN model performance graph: model architecture (a), training and testing regression (b), model error histogram (c).

4.4.1. Developed blast-induced ground vibration ANN model

ANN model with 2:4:1 architecture was built based on the approach explained in section 3.1 using a hybrid algorithm. Fig. 9 presents the prediction regression for both the training and testing dataset. The model with $R^2 = 0.998$ and $MSE = 0.00207$ was adopted for blast-induced noise prediction and for obtaining the optimum charge weight per drill hole based on the *MIC* and the maximum safety distance. The blast-induced noise formula is found in Equation (11)–(15) by the best ANN model, where the R^2 values are 99.99% and 99.8% for the training and testing dataset, respectively. The proposed model was found suitable for predicting the noise level in a limestone quarry for pre-blast design.

$$GV = 1.699 \tanh\left(\sum_{i=1}^{4} Xi + 0.22861\right) + 1.949 \quad (11)$$

$$X_1 = 0.2905\tanh\,(2.3050MIC - 1.3936D - 2.7163) \quad (12)$$

$$X_2 = 0.25599\tanh\,(2.5599MIC - 0.9922D - 0.8364) \quad (13)$$

$$X_3 = 0.56826\tanh\,(2.6430MIC + 1.19591D + 0.64889) \quad (14)$$

$$X_4 = 0.31372\tanh\,(-2.07471MIC - 1.8803D - 2.79993) \quad (15)$$

5. Optimized blast variable for sustainable dolomite mining

One of the most influential parameters on blast-induced effects is blast charge per delay, as noted by Armaghani et al. [46]. The proposed models were used to improve the quantity of explosive used per initiation in the case study limestone mine, thereby optimizing blast-induced effects. Minimizing the MIC and establishing the corresponding FEPA threshold limit noise and ground vibration level required determining the minimum and maximum blast effective distance from the observed blast round and utilizing the proposed models. Table 4 displays the results of applying the proposed models to reduce mine explosive use to a safe level. The MIC's detection range was found to be between 68.46 and 147.2 dB at a distance of 0.28–1.89 mm, with a minimum detection weight of 800–1200 kg. Four blast rounds were used to verify the fragmentation result at the two threshold levels. By employing WipFrag Software, we were able to analyze the fragmentation of the proposed *MIC* limit for dolomite mining. As shown by the particle size distribution curve in Fig. 8 and the results in Table 5, the analysis showed that *MIC* = 800 Kg yielded large boulders (Fig. 10). Fig. 10 displays the results of the *MIC* = 1200 Kg blast, which also showed a significant number of fine materials. At 1 Km observation distance, the optimum *MIC* = 1100 Kg was found with the noise level and ground vibration of 120.6 dB and 1.82 mm, 92.74 dB and 1.53 m, respectively (Table 4). The proposed ANN models enabled a reduction in mine blast production and safety from an unsustainable level of ground vibration and noise to below the FEPA threshold limit.

Table 4. Optimized MIC and observation safety distance predicted with the ANN extracted equation.

MIC (Kg)	Observation distance (m)	Noise level (dB)	Ground vibration (mm)
1200 (Max)	1025	147.2	1.89
1100 (Optimum)	1000	120.6	1.82
800	600	68.46	0.28
500	500	64.06	0.41
800	1025	54.82	0.19
500	1000	34.64	0.06
1200	600	118.42	2.01
1100	500	92.74	1.53

6. Comparison of the proposed ANN model with USBM and other rule of thumb equations

The ground vibration and noise level measured from the six testing blast rounds were compared with the predicted values from the developed ANN models and other existing empirical models, including USBM and McKenzine [47]) (Eq. (16)–(7)) noise level prediction models. The peak level of ground vibration at any given point during the blast rounds was determined using USBM Eq. (18) [48].

$$dB = 165 - (24\mathrm{Log}(D/W^{1/3}) \quad (16)$$

$$dB = H(D/Q^{1/3})^{-\beta} \quad (17)$$

$$PPV = K(D/W_d^{1/2})^{-B} \quad (18)$$

Where: D is the observation distance in m, and W_d is the maximum explosive charge in Kg, $H = 0.515$, $\beta = 622$, $K = 1.37$, and $B = -0.183$ are the site and geological constant factors, respectively. The site factors are determined by plotting the logarithmic plot of *PPV* versus scaled distance. The straight-line best representing the data has a negative slope B

Table 5. Fragmentation result after ANN optimization.

Size (mm)	Blast 1	Blast 2	Blast 3	Blast 4	Blast 5	Blast 6
	MIC = 1200 Kg	*MIC* = 1100 Kg	*MIC* = 500 Kg	*MIC* = 1200 Kg	*MIC* = 1100 Kg	*MIC* = 500 Kg
20	0	0.4	0.05	0	0.4	0.05
25	0.024	0.59	0.27	0.024	0.59	0.27
50	0.34	1.96	1.45	0.34	1.96	1.45
75	1.31	3.94	4.06	1.31	3.94	4.06
100	3.16	6.43	7.78	3.16	6.43	7.78
250	29.51	28.07	36.18	29.51	28.07	36.18
300	39.88	36.42	41.62	39.88	36.42	41.62
350	49.21	44.73	48.61	49.21	44.73	48.61
400	57.17162	52.69869	53.3	57.17162	52.69869	53.3
450	63.79	60.13	55.59	63.79	60.13	55.59
500	64.02	60.68	56.02	64.02	60.68	56.02

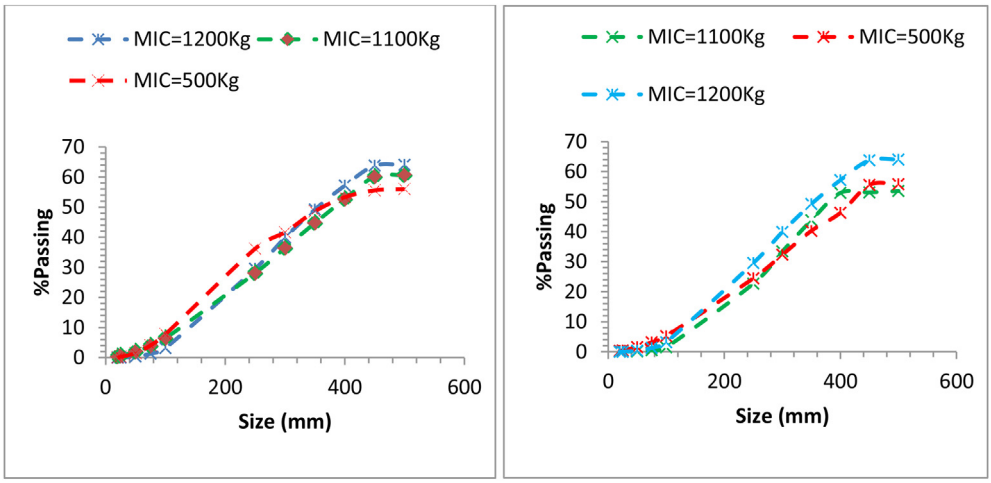

a. Blast 1-3 *b. Blast 4-6*

Fig. 10. Fragmentation analysis result after ANN optimization.

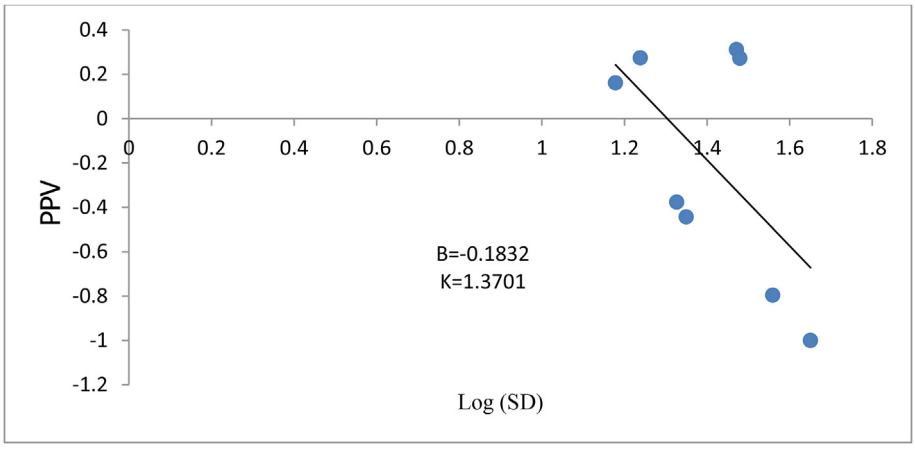

Fig. 11. PPV and scaled distance on log-log scale for USBM.

and an intercept (Fig. 11). The USBM model was used based on the mine site geological condition and blast design as considered in Fig. 12 for the determination of the site-specific parameters.

Comparisons were made between the models developed in the proposed study (ANN) and those suggested in the literature (USBM predictor and McKenzine [47]) for the prediction of blast-induced

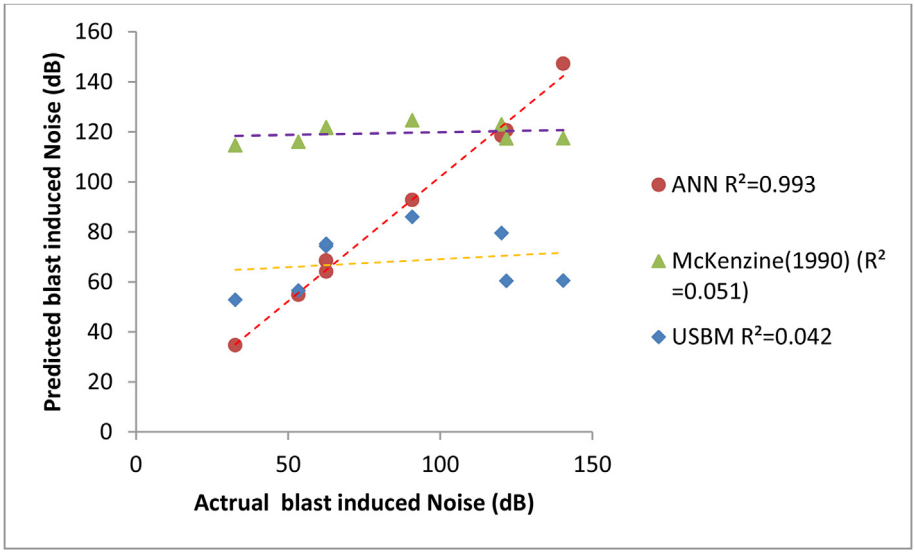

Fig. 12. Relationship between the actual blast-induced noise and the predicted.

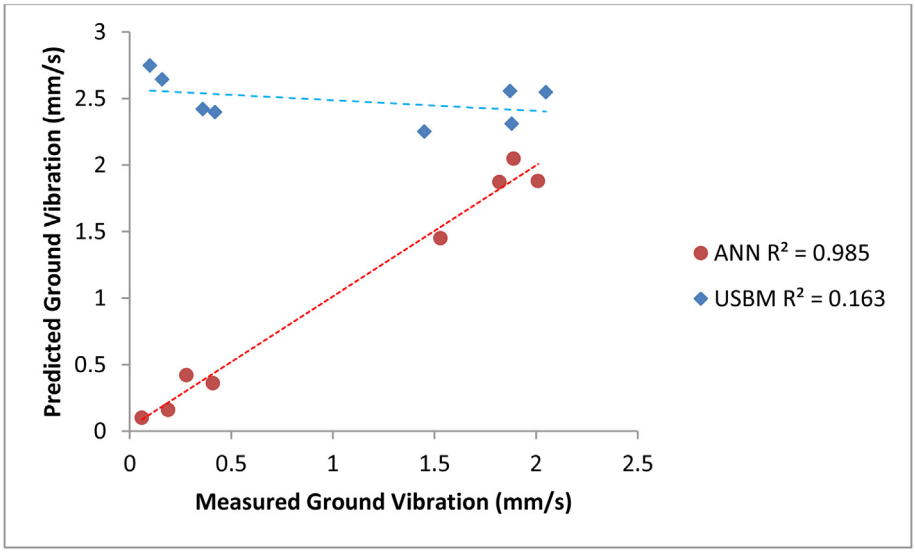

Fig. 13. Relationship between the actual blast-induced ground vibration and the predicted.

effects. The USBM and McKenzine [47] models have R^2 values of 0.042 and 0.051, respectively, for their predictions of the noise level, while the ANN has an R^2 value of 0.993. Compared to the two existing models, the proposed ANN model provides more accurate forecasts of blast-induced noise. On the other hand, the USBM has a low R^2 value for predicting blast-induced ground vibration (0.163), while the ANN used in the current study has a much higher value (0.985) (Fig. 13).

7. Conclusions

A wide range of environmental impacts can be caused by mining activities due to the alteration of landform that occurs during excavation. The process of fragmenting the rock mass into smaller sizes begins with blasting activities, which involve the use of explosives and blasting accessories. Explosives for blasting have other environmental consequences, such as ground vibration and noise generation, which need to be properly investigated to achieve sustainable mining. This research examined the effects of blast charges and other factors on the environment of limestone quarries. The positive correlation between limestone moisture content and strength property found in the rock strength and moisture content results [49] suggests that rock strength facilitates acid mine drainage infiltration

both during mining and after the mine has been abandoned. Blast-induced ground vibration and noise level were found to be affected by maximum instantaneous charge and instrument measuring distance.

From the study results the following conclusions can be drawn:

1) According to the rock property analyses, the limestone has average water absorption of 8.8%, a density of 2.41 g/cm^3 and a uniaxial compressive strength of 90 MPa. According to the Bieniawski rock *UCS* rating, the limestone in the case study is classified as strong limestone. The analysis also reveals that the formation moisture content is affected by the rock strength properties.
2) The maximum initiated explosive charge in the limestone quarry blast site ranges from 580 kg to 1600 kg, as evaluated from several blast round operations. It was deduced that the maximum explosive instantaneous charge has a directly proportional relationship with the blast after ground vibration and induced noise level.
3) The Noise level and ground vibration measured in the limestone quarry blast site using V90 seismograph ranges within, 3.5 dB to 15.8 dB and 0.25 mm/s to 3.6 mm/s respectively. It was revealed that the limestone quarry blast impact has lower values as compared with the Federal environment protection agency (FEPA) threshold limits.
4) The proposed ANN models developed have high prediction accuracy and can be used to estimate the blast-induced effect for sustainable limestone mining operations.

The authors' future work will concentrate on predicting the blast-induced ground vibration and noise level using other Machine learning techniques and deep learning modeling techniques with additional data from other mines to widen the model application in other industrial rock extraction projects.

Ethical statement

Authors state that the research was conducted according to ethical standards.

Funding body

This research received no external funding.

Conflicts of interest

The authors declare no conflict of interest.

Acknowledgements

None.

References

[1] Kanchibotla SS, Valery W, Morrell S. Modelling fines in blast fragmentation and its impact on crushing and grinding. In: Explo '99–A conference on rock breaking. Kalgoorlie, Australia: The Australasian Institute of Mining and Metallurgy; 1999, November. p. 137–44.
[2] Jhanwar JC. Theory and practice of air-deck blasting in mines and surface excavations: a review. Geotech Geol Eng 2011;29(5):651–63.
[3] Taiwo BO. Effect of charge load proportion and blast controllable factor design on blast fragment size distribution. J Brilliant Eng 2022;3:4658.
[4] Kumar R, Choudhury D, Bhargava K. Determination of blast-induced ground vibration equations for rocks using mechanical and geological properties. J Rock Mech Geotech Eng 2016;8(3):341–9.
[5] Choudhary BS, Agrawal A. Minimization of blast-induced hazards and efficient utilization of blast energy by implementing a novel stemming plug system for eco-friendly blasting in open pit mines. Nat Resour Res 2022;31(6):3393–410.
[6] Agrawal A, Choudhary BS, Murthy VMSR, Murmu S. Impact of bedding planes, delay interval and firing orientation on blast induced ground vibration in production blasting with controlling strategies. Measurement 2022;202:111887.
[7] Deniz V, Deniz OT. The environmental effects of the air shock generated by blasting. Mugla J Sci and Technology 2017;3(2):166–70.
[8] Ainalis D, Kaufmann O, Tshibangu JP, Verlinden O, Kouroussis G. Assessing blast source pressure modelling approaches for the numerical simulation of ground vibrations. In: Proceedings of the 23rd international congress on sound and vibration; 2016. Athens (Greece), July 10-14, 2016.
[9] Baranov EG, Bondarenko IF, Vedin AT. Mining and industrial applications of low density explosives. CRC Press; 1996.
[10] Mortazavi A. Using discontinuous deformation analysis. Doctoral dissertation, Queen's University Kingston; 1999.
[11] Cullis IG. Blast waves and how they interact with structures. BMJ Military Health 2001;147(1):16–26.
[12] Resende R, Lamas L, Lemos J, Calçada R. Micromechanical modelling of stress waves in rock and rock fractures. Rock Mech Rock Eng 2010;43(6):741–61.
[13] Dumakor-Dupey NK, Arya S, Jha A. Advances in blast-induced impact prediction—a review of machine learning applications. Minerals 2021;11(6):601.
[14] Jaffar N, Abdul-Tharim AH, Mohd-Kamar IF, Lop NS. A literature review of ergonomics risk factors in construction industry. Procedia Eng 2011;20:89–97.
[15] Cleary PW, Sawley ML. DEM modelling of industrial granular flows: 3D case studies and the effect of particle shape on hopper discharge. Appl Math Model 2002;26(2):89–111.
[16] Michelsen A. Physical aspects of vibrational communication. In: Studying vibrational communication. Berlin, Heidelberg: Springer; 2014. p. 199–213.
[17] Bansah KJ, Kansake BA, Dumakor-Dupey NK. Baseline structural assessment: mechanism for mitigating potential conflicts due to blast vibration. In: 4th UMaT biennial international mining and mineral conference; 2016. p. 42–8.
[18] Díaz J, Ruiz M, Sánchez-Pastor PS, Romero P. Urban seismology: on the origin of earth vibrations within a city. Sci Rep 2017;7(1):1–11.
[19] Valdivia C, Vega M, Scherpenisse CR, Adamson WR. Vibration simulation method to control stability in the northeast corner of escondia mine. Int. J. Blast. Fragment. 2003;7:63–78.
[20] Rossmanith HP, Hochholdinger-Arsic V, Uenishi K. Understanding size and boundary effects in scaled model blast-plane problems. Int. J. Blast. Fragment 2005;9:93–125.

[21] Bhandari S, Balkema AA. Engineering rock blasting operations. Rotterdam: Netherlands/Brookfield, USA Publishers; 1997. p. 400.
[22] Banadaki MD, Mohanty B. Numerical simulation of stress wave induced fractures in rock. Int J Impact Eng 2012;40: 16–25.
[23] Alessandro G, Marilena C, Vladisla K. An assessment of blasting vibrations: a case study on quarry operation. Am J Environ Sci 2009;5(4):468–74.
[24] Mpofu M, Ngobese S, Maphalala B, Roberts D, Khan S. The influence of stemming practice on ground vibration and air blast. J S Afr Inst Min Metall 2021;121(1):1–10.
[25] Ranjan K, Deepankar C, Kapilesh B. Determination of blast-induced ground vibration equations for rocks using mechanical and geological properties. J Rock Mech Geotech Eng 2016;8:341–9.
[26] Roy MP, Singh PK, Sarim M, Shekhawat LS. Blast design and vibration control at an underground metal mine for the safety of surface structures. Int J Rock Mech Min Sci 2016;83: 107–15.
[27] Cheng R, Zhou Z, Chen W, Hao H. Effects of axial air deck on blast-induced ground vibration. Rock Mech Rock Eng 2022;55(2):1037–53.
[28] Trivedi R, Singh TN, Mudgal K, Gupta N. Application of artificial neural network for blast performance evaluation. Int J Renew Energy Technol 2014;3(5):564–74.
[29] Ragam P, Nimaje DS. Evaluation and prediction of blast-induced peak particle velocity using artificial neural network: a case study. Noise Vib Worldw 2018;49(3):111–9.
[30] Lawal AI. An artificial neural network-based mathematical model for the prediction of blast-induced ground vibration in granite quarries in Ibadan, Oyo State, Nigeria. Scientific African 2020;8:e00413.
[31] Zhu C, Xu Y, Wu Y, He M, Zhu C, Meng Q, et al. A hybrid artificial bee colony algorithm and support vector machine for predicting blast-induced ground vibration. Earthq Eng Eng Vib 2022;21(4):861–76.
[32] Qiu Y, Zhou J, Khandelwal M, Yang H, Yang P, Li C. Performance evaluation of hybrid WOA-XGBoost, GWO-XGBoost and BO-XGBoost models to predict blast-induced ground vibration. Eng Comput 2022;38(5):4145–62.
[33] Etikan I, Bala K. Sampling and sampling methods. Biom Biostat Int J 2017;5(6):215–7. https://doi.org/10.15406/bbij.2017.05.00149.
[34] ISRM. International society for rock Mechanics. Rock characterization, testing and monitoring. In: Brown ET, editor. ISRM suggested methods. Commission on testing methods, international society for rock Mechanics (ISRM). Oxford, UK: Pergamon Press; 1981. p. 75–105.
[35] Stagg MS, Engler AJ. Measurement of blast-induced ground vibrations and seismograph calibrationvol. 8506. US Department of the Interior, Bureau of Mines; 1980.
[36] Lawal AI, Aladejare AE, Onifade M, Bada S, Idris MA. Predictions of elemental composition of coal and biomass from their proximate analyses using ANFIS, ANN and MLR. Int J Coal Science and Technology 2021;8(1):124–40. https://doi.org/10.1007/s40789-020-00346-9.
[37] Maerz NH. Image sampling techniques and requirements for automated image analysis of rock fragments. In: Proceedings of ISRM/fragblast 5 workshop and short course on fragmentation measurement. Montreal: A. A. Balkema; 1996.
[38] Taiwo BO. Improvement of small-scale dolomite blasting productivity: comparison of existing empirical models with image analysis software and artificial neural network models. Journal of Mining and Environment 2022;13(3):627–41.
[39] Bieniawski ZT. Engineering rock mass classifications. In: A complete manual for engineers and geologists in mining, civil and petroleum engineering. Toronto: John Wiley & Sons; 1989. Bishop, A. (1955). The Use of the Slip Circle in the Stability Analysis of Slopes. Géotechnique 5.1: 7-17.
[40] Lefebvre R, Hockley D, Smolensky J, Gélinas P. Multiphase transfer processes in waste rock piles producing acid mine drainage: 1: conceptual model and system characterization. J Contam Hydrol 2001;52(1–4):137–64.
[41] Afeni TB, Osasan SK. Assessment of noise and ground vibration induced during blasting operations in an open pit mine—a case study on Ewekoro limestone quarry, Nigeria. Min Sci Technol 2009;19(4):420–4.
[42] Nguyen VD, Lee CW, Bui XN, Nguyen H, Tran QH, Long NQ, et al. Evaluating the air flow and gas dispersion behavior in a deep open-pit mine based on monitoring and cfd analysis: a case study at the coc sau open-pit coal mine (Vietnam). In: Proceedings of the international conference on innovations for sustainable and responsible mining. Cham: Springer; 2021. p. 224–44.
[43] Yang J, Sun J, Jia Y, Yao Y. Energy generation and attenuation of blast-induced seismic waves under in situ stress conditions. Appl Sci 2022;12(18):9146.
[44] Zhi-qiang Yin Z, Ze-di W, Guang-ming Z, Ma Hai-feng Z, Rui-min F. Assessment of blasting-induced ground vibration in an open-pit mine under different rock properties. Adv Civ Eng 2018;2018. https://doi.org/10.1155/2018/4603687. Article ID 4603687, 10 pages.
[45] Mesec J, Kovač I, Soldo B. Estimation of particle velocity based on blast event measurements at different rock unit. Soil Dynam Earthq Eng 2010;30(10):1004–9.
[46] Armaghani DJ, Hajihassani M, Mohamad ET, Marto A, Noorani SA. Blasting-induced flyrock and ground vibration prediction through an expert artificial neural network based on particle swarm optimization. Arabian J Geosci 2014;7(12): 5383–96.
[47] McKenzie C. Quarry blast monitoring: technical and environmental perspectives. Quarry Manag 1990;17:23–34.
[48] Tiile RN. Artificial neural network approach to predict blast-induced ground vibration, airblast and rock fragmentation. Missouri University of Science and Technology; 2016.
[49] Nishimoto N, Yamamoto Y, Yamagata S, Igarashi T, Tomiyama S. Acid mine drainage sources and impact on groundwater at the osarizawa mine, Japan. Minerals 2021; 11(9):998.